Novel polypyrrole-graphene oxide-gold nanocomposite for high performance hydrogen peroxide sensing application

D. Mathivanan[a], K.S. Shalini Devi[b], G. Sathiyan [a], Ankit Tyagi[a], V. A.O. P. da Silva[c], B. C. Janegitz[c], Jai Prakash[a,d*]and R. K. Gupta[a,e*]

[a]Department of Chemical Engineering, Indian Institute of Technology Kanpur, Kanpur 208016, India
[b]School of Chemical and Biotechnology, Centre for Nanotechnology & Advanced Biomaterials (CeNTAB), SASTRA University, Thanjavur-613401, India
[c]Department of Nature Sciences, Mathematics and Education, Universidade Federal de São Carlos, Araras, São Paulo, 13600-970, Brasil
[d]Department of Chemistry, National Institute of Technology Hamirpur, Hamirpur-177005, India
[e]Center for Environmental Science and Engineering, Indian Institute of Technology Kanpur, Kanpur 208016, India

Abstract

Hydrogen peroxide (H_2O_2) plays a major role in the signaling processes in various diseases and its qualitative or quantitative analyses are of paramount importance in healthcare, process, and food, etc. In this study, an electrochemical ultra-high sensor has been reported for the detection of H_2O_2 based on nanocomposites consisting of polypyrrole (PPy), graphene oxide (GO), and gold nanoparticles (AuNPs). These nanocomposites were studied using scanning electron microscopy, ultraviolet-visible, Fourier transform infrared, Raman spectroscopies and cyclic voltammetry techniques. The obtained final electrode (PPy-GO-AuNPs/GCE) showed high electrocatalytic activity towards H_2O_2 allowing the detection of H_2O_2 at a negative potential at the range of -20 V *vs*.Ag/AgCl. The amperometric response of the non-enzymatic H_2O_2 sensor exhibited a higher sensitivity of 41.35 µA/mM at linear range around 2.5-25 mM, and a low detection limit of 5 µM (S/N= 3). The practical applicability of nanocomposites was also investigated for H_2O_2 sensing in real milk. These results suggest that PPy-GO-AuNPs/GCE nanocomposite is promising and effective for low concentration detection with higher sensitivity and wider linear response range as compared to the previously reported H_2O_2 sensors. Furthermore, these nanocomposites show higher stability, repeatability and reproducibility of the sensing data indicating their potential as long term practical applications.

Keywords: Conducting polymer; gold nanoparticles; nanocomposite; graphene oxide; H_2O_2 sensing

***Corresponding authors email:** JP (jai.gupta1983@gmail.com, jaip@nith.ac.in) and RKG (guptark@iitk.ac)

1. Introduction

Hydrogen peroxide (H_2O_2), a signaling molecule is mostly involved in numerous physiological and pathological functions such as cell proliferation, cell migration, circadian rhythm, the fast, reliable, and immune response.[1, 2] A precise detection of H_2O_2 has gained considerable attention because it plays a vital mediator role in food, clinical, pharmaceutical, and environmental analysis.[3] Nowadays, numerous approaches have been explored to detect H_2O_2, such as spectrometry,[4] fluorometry,[5] chromatography,[6] chemiluminescence[7], and electrochemical methods, etc.[8] Out of these, the electrochemical technique has been widely used for the detection of H_2O_2 because of its simplicity, fast response, accuracy, and economically better efficiency for analysis. The electrochemical method has several advantages over traditional methods such as reasonably fabrication, an easy-to-make, more sensitive and also cost-effective compare to traditional methods.

There are two types of sensors such as enzyme and non-enzyme based sensors, which are frequently used for H_2O_2 sensing. Even though the enzyme-based sensors have shown excellent results in sensing applications, also have some drawbacks such as complex enzyme immobilization processes, high cost and these sensors are easily influenced by the various parameters such as pH, temperature, etc.[9] Currently, research is mainly focused on non-enzyme electrocatalytic sensors in order to overcome such issues. In this case, mainly conducting polymers such as polypyrrole (PPy), oxide-based catalysts and nanoparticles (NPs) have been generally considered for highly efficient sensing applications.[10, 11] PPy is an important conducting polymers as it follows a very simple synthesis process, has excellent redox and higher conducting properties along with better environmental stability. The specific properties of PPy are exposed for various technological approaches, such as chemical/biochemical sensing, rechargeable batteries, and electronic devices etc.[12] PPy has strong electronic interaction towards the metallic NPs within the polymer matrix.[13-16] Metal NPs such as Ag, Au, and Pt have been broadly used for fabricating different kinds of sensors[17-19]. AuNPs have been reported for exhibiting interesting features for various applications including nanoelectronics, sensors, optics, and catalysis etc. due to their excellent properties such as electronic conductivity, chemical stability, biocompatibility, mechanical resistance, and large areas of the active surface[20-22]. It is expected that the use of AuNPs can improve sensing performance due to its excellent electrocatalytic activity towards H_2O_2.[23-26] Similarly, graphene is an important functional nanomaterial with excellent sensing properties

which is an atom thick two-dimensional nanostructure with sp^2 bonded carbon atoms in a honeycomb crystal lattice with remarkably high crystal quality and electronic properties.[27-29] After the discovery of graphene, various forms of graphene have been explored in nanotechnology research like graphene oxide (GO) and reduced graphene oxide (RGO), and have been used as key sensor units to combine with other inorganic nanomaterials and biomolecules to fabricate biosensors with high performance.[30, 31]. Also, the use of GO within AuNPs are interesting alternatives for electrochemical sensing, which can when used together, lead to synergic effects, high electrical conductivity, large surface area, and biocompatibility. Please, cite https://doi.org/10.3390/ma9060406

In this present study, we have synthesized PPy-GO-AuNPs nanocomposites implementing a simple and cost-effective technique i.e. *in situ* polymerization techniques using ferric chloride hexahydrate ($FeCl_3 \cdot 6H_2O$) as an oxidizing agent. These nanocomposites with different compositions were studied with detailed preparation and characterization methods for promising H_2O_2 sensing applications. The synthesized nanocomposites exhibited excellent structural and optical properties at the optimized compositions of AuNPs. This study revealed that the developed sensing nanomaterials showed higher sensitivity along with the low limit of detection and wider linear response range for H_2O_2 as compared to the previously reported H_2O_2 sensors. Also, these nanocomposites showed higher stability, repeatability, and reproducibility of the data indicating their potential as long-term sensing applications.

2. Materials and methods

2.1. Chemicals and reagents

Pyrrole monomers (99.5%), GO, AuNPs, Nafion, ethanol (99%), acetone (99%), and ferric chloride hexahydrate ($FeCl_3 \cdot .6H_2O$, 99%) were borrowed from Sigma Aldrich. Di-sodium hydrogen phosphate anhydrous (Na_2HPO_4, 99%), sodium dihydrogen phosphate dihydrate ($NaH_2PO_4.2H_2O$, 99%)) and hydrogen peroxide (30% in 500 mL) were purchased from Merck.

2.2. Synthesis of PPy

PPy was synthesized by chemical polymerization technique using ferric chloride as an oxidant.[32] Around 1.5 mL of pyrrole was taken into a round bottom (RB) flask followed by the addition of 20 mL ethanol with constant stirring. Then, $FeCl_3 \cdot 6H_2O$ (9.0 g, 33 mmol) was dissolved in 200 mL of ethanol and it was added into the above reaction mixture dropwise. The reaction mixture was continued to stirrer at normal conditions for about 24 hrs. It resulted in black color after the complete mixing of pyrrole and $FeCl_3$ solution. The resulted solution was filtered followed by washing simultaneously using water and acetone to remove the unreacted pyrrole and excess of ferric chloride. The resultant product was dried at 80 °C for 12 h as schematically shown in **Fig. S1.**

2.3. Synthesis of PPy-GO-AuNPs nanocomposites

PPy-GO-AuNPs nanocomposites were synthesized as mentioned in the last section 2.2. Around 1.5 mL of pyrrole was poured into the RB flask and around 20 mL of ethanol was added with constant stirring followed by different concentrations like1, 3,5, and 7 mL (0.02 mg/mL) of AuNPs, and 0.3 g of GO were added and stirred well. Then, $FeCl_3 \cdot 6H_2O$ (9.0 g 33 mmol) was dissolved in 200 mL of ethanol added into the above reaction mixture resulting in a black solution. Further steps were followed as mentioned above and more details are given in supporting information. The synthesis of PPy-GO-AuNPs nanocomposite is shown in **Fig. 1.**

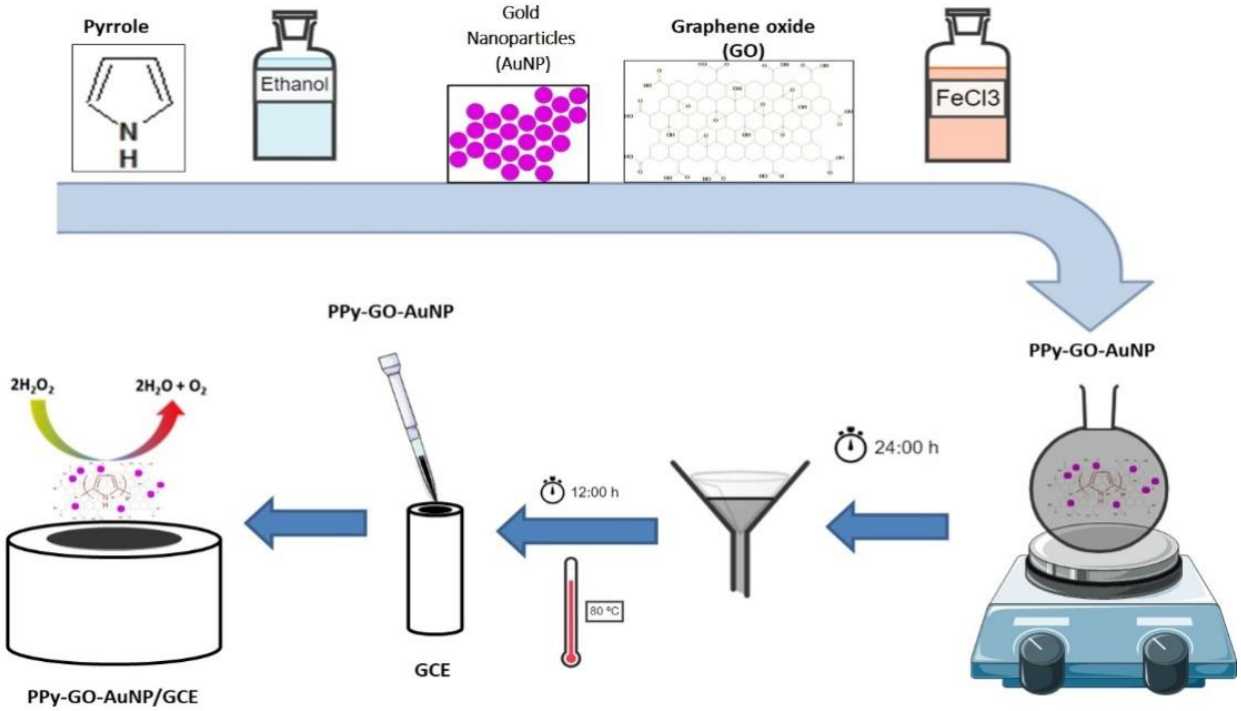

Fig. 1 Synthesis of PPy-GO-AuNPs nanocomposites

2.4. Characterization

The obtained multi-element composite nanomaterials were characterized by using multi-techniques. The Fourier transform infrared (FT-IR) (from Perkin Elmer, USA), UV-visible, and Raman spectrometers (from WiTec, Germany) were used to analyze the chemical, electronic, and optical properties of all the samples. The surface morphology of the synthesized composite nanomaterial was carried out using a field emission scanning electron microscope (FE-SEM from Quanta 200, Zeiss, from Germany). The compositional analysis of the polymer composites was evaluated by using energy-dispersive X-ray spectroscopy (EDX linked to FE-SEM, Oxford Instrument, UK).

2.5. Electrochemical characterization

The electrochemical measurements were performed at room temperature in the Metrohm Autolab (PGSTAT302N) cyclic voltammetry (CV) set up. A well-established three-electrode cell was used for electrochemical analysis. The cell was equipped with a glassy carbon electrode (GCE) which was used as a working electrode, aAg/AgCl electrode which was used as a reference electrode, and a platinum wire which was used as an auxiliary electrode. The phosphate buffer solution (PBS, 0.1 M) was used as an electrolyte, prepared with Na_2HPO_4 and NaH_2PO_4. Then the pH (2.0 – 10) was adjusted using sodium hydroxide and acetic acid.

2.6. Fabrication of electrode

The GCE was polished and washed with alumina powder and distilled water respectively. It was then sonicated in ethanol and further in distilled water followed by drying in the steam of N_2. Around 1 mg of PPy composites or nanocomposites with different concentrations of AuNPs were dissolved with 800µL of ethanol and 200µL of nafion. 5 µL of each (1.0 µg/mL) was applied on the surface of GCE and dried under visible light.

3. Results and discussion

3.1 PPy-GO composites with different composition of Au NPs

As discussed in section 2.3 and shown in Fig.1**,** the PPy-GO-AuNPs nanocomposites were prepared with different Au concentrations such as 1, 3,5 and 7 mL (0.02 mg/mL) of AuNPs. Amongst the various compositions, PPy-GO-AuNPs nanocomposite with 5 mL AuNPs

concentration showed excellent sensitivity as shown in **Table S1**. The CV results for all the compositions are discussed and provided in Supporting Information (**Fig. S2-S5**). Since nanocomposite with 5 mL AuNPs concentration showed better performance in H_2O sensing, we have discussed here all the physo-chemical properties including sensing performance of PPy-GO-AuNPs nanocomposite with only 5 mL AuNPs concentration.

3.2 UV analysis

Absorption spectra of PPy and PPy-GO-AuNPs (5 mL) nanocomposite are shown in **Fig. 2.** The absorption band observed at 273 nm shows the characteristic of PPy which corresponds to the π–π* transitions for C=C or C=N groups (**Fig.2[A])**.[33] In **Fig. 2 [B**], a blue shift can be observed in the absorption band from 273 nm to 254 nm that may be attributed to the incorporation of GO in PPy. That means the energy of π-π* transitions between the PPy-GO changes significantly by the addition of GO, which happens most probably due to theπ-π stacking between PPy and GO.[34] The absorption spectrum of PPy-GO-Au nanocomposites shows the presence of Au NPs i.e. the dual peak at 459 nm and 562 nm, adsorbed on PPy-GO nanocomposites (**Fig. 2[C])**.[35] It indicates the surface plasmon resonance properties of AuNPs present in the nanocomposite.

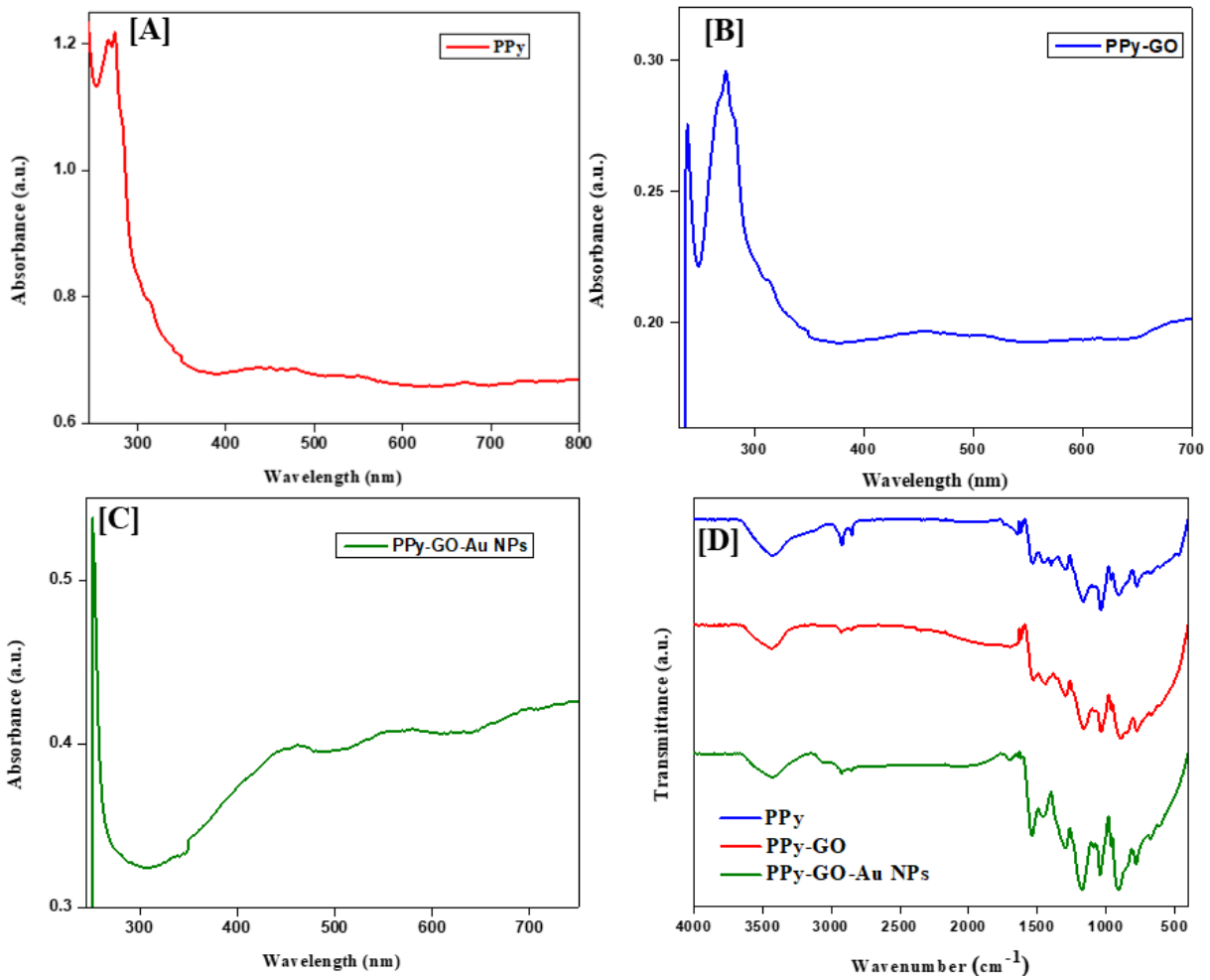

Fig. 2 Absorption spectra of **[A]** PPy, **[B]** PPy-GO composites and **[C]** PPy-GO-AuNPs nanocomposites. **[D]** Comparable FT-IR spectra of the same.

3.3. FT-IR spectroscopy

Fig. 2 [D] shows the FTIR spectra of PPy, PPy-GO, and PPy-GO-AuNPs (5 mL) nanocomposites. The absorption bands at 1544, 1447,1297, 1169, 1040 and 913 cm^{-1} show characteristic of PPy.[13, 36] The bands at 1544cm^{-1} and 1447 cm^{-1}vibrations correspond to the pyrrole ring. The bands at 1297 and 913 cm^{-1} correspond to =C–H in-plane and =C–H out-of-plane vibrations respectively.[36] Moreover, the absorption band corresponds C–N stretching is observed at 1128 cm^{-1}. Similar trends have been observed for composite samples i.e. PPy-GO and PPy-GO-AuNPs nanocomposite along with a slight shift in their vibrational frequencies either blue or red shift[37] indicating the better interaction of components. Although, there is a solid electrostatic interface among the AuNPs with PPy coated GO surfaces.[38] The broadbands appeared at 3425 cm^{-1} and the spectra at 2922 cm^{-1} resemble N–H and C–H stretching vibration in PPy-GO-AuNPs nanocomposites which may be attributed to the interaction of Au NPs with PPy

and GO surfaces. The interaction of GO with the polypyrrole complex is clear from the slight shift in the vibrational frequencies which might due to the oxygen functional groups present in the edges of GO.

3.4. Raman spectroscopy Analysis

Fig. 3 shows the Raman spectra of polymer and nanocomposite samples. The observed bands at 1333 and 1584 cm^{-1} show the characteristic of PPy corresponding to the ring stretching mode and C=C backbone stretching respectively.[39]

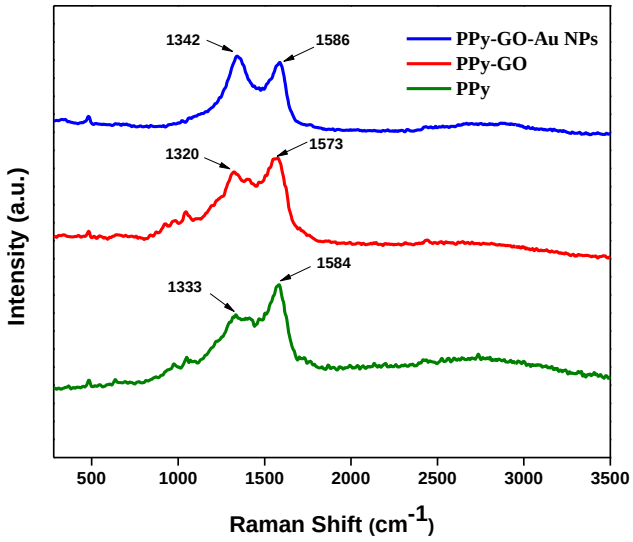

Fig. 3: Raman spectra of PPy, and PPy-GO, PPy-GO-AuNPs nanocomposites.

The band around 1048 cm^{-1} indicates the C–H in-plane deformation. The bands at 976 cm^{-1} and 874 cm^{-1} correspond to the quinoid bipolaronic and polaronic structures, respectively.[40] The D band and G band of PPy-GO are shifted to 1342 cm^{-1} and 1586 cm^{-1} for PPy-GO-AuNPs. The increased relative intensity of D bands exhibits the strong interaction of PPy monomer with GO and Au. Similarly, shifting appeared as a result of π–π interactions of PPy and GO and strong interaction with AuNPs.[41, 42]

3.5. SEM-EDX analysis

The SEM micrographs of PPy, PPy-GO and PPy-GO-AuNPs (5 mL) nanocomposites are shown in **Fig. 4**. The SEM image of PPy exhibits a cauliflower-like or tumor-like structure. It can be seen clearly that the abundance of PPy particles has been grown and GO layers and seems to be coated on the surface as shown in **Fig. 4[B]**. It confirms the formation of PPy-GO nanocomposite. In

the case of PPy-GO-AuNPs nanocomposite, it seems like AuNPs and GO are entangled inside the polymer layer **(Fig. 4[C])** as AuNPs cannot be seen clearly in SEM image of nanocomposites.

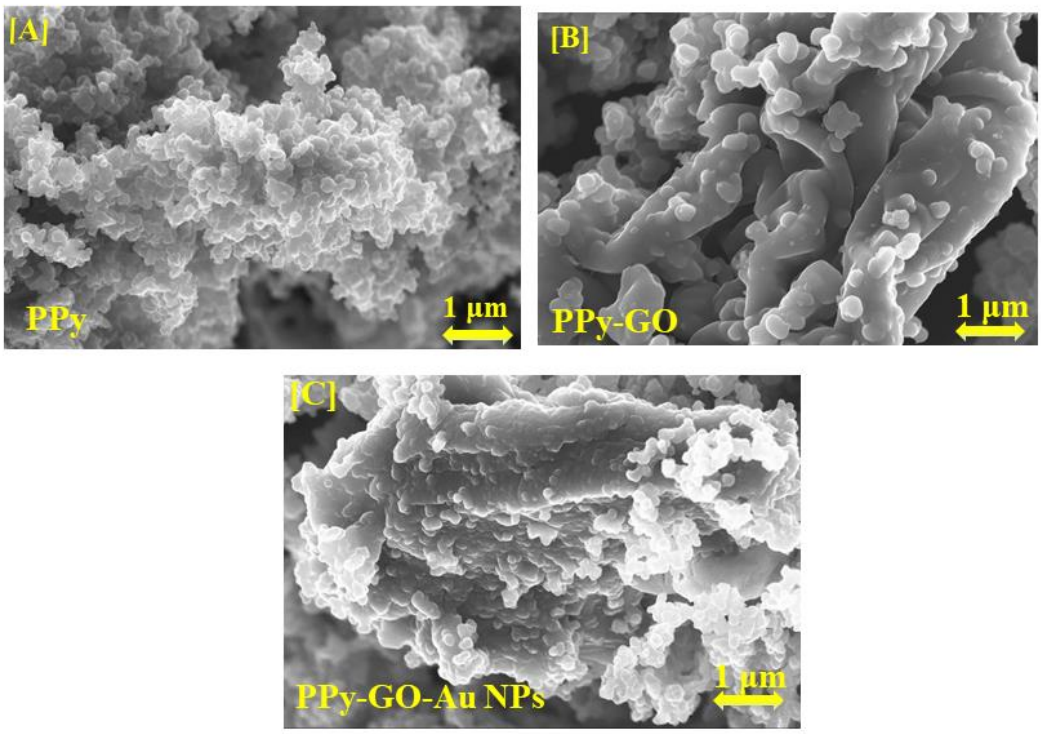

Fig 4. SEM micrographs of **[A]** PPy; **[B]** PPy-GO; **and [C]** PPy-GO-AuNPs (5 mL) nanocomposite

Also, GO forms a layer-by-layer, network structure with denser stacking amid the polymerization technique. The energy dispersive X-ray Diffractive (EDX) analysis of PPy-GO-AuNPs nanocomposite was carried out to determine elemental composition as shown in Supporting Information which indicates the presence of various components such as C, O, and Au in nanocomposites (**Fig. S6**).

3.6. H_2O_2 sensing behavior of PPy-GO-AuNPs nanocomposites

The sensing behavior of PPy-GO-AuNPs nanocomposite as discussed above towards H_2O_2 was studied through the electrocatalytic activity of PPy-GO-AuNPs/GCE using CV set up. The CV curves of PPy-GO-AuNPs/GCE in 0.1 M phosphate-buffered saline (PBS) solution at pH 7 with the potential ranging from −1.0 V to 0.2 V *vs.* Ag/AgCl at a scan rate of 20 mV/s are shown in **Fig. 5 [A]**. The absence of any peak response in the case of GCE and PPy-GO-AuNPs/GCE exhibits their inactive nature for any electrocatalytic activity in this potential range.[43] **Fig. 5 [B]**

indicates the CV curves at different scan rates of 10-100 mV/s for the nanocomposites in the same PBS solution with 2.5 mM H_2O_2.

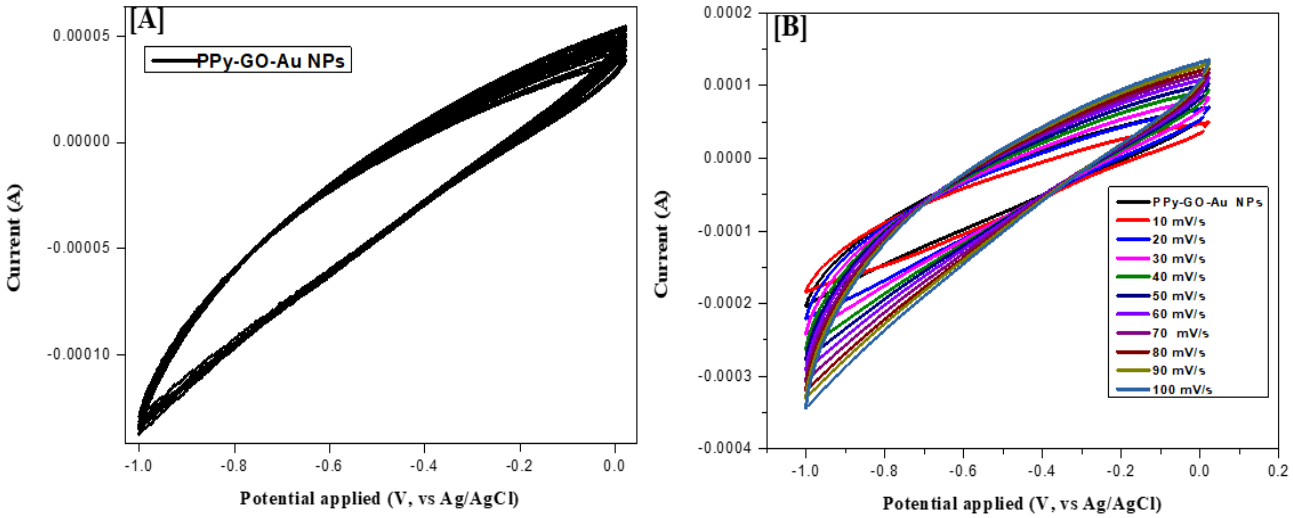

Fig. 5. (A) CV curves of PPy-GO-AuNPs/GCE in 50 ml 0.1 M PBS solution at pH 7 at a scan rate of 20 mV/s for 10 cycles in the range of scanning potential from -1.0 V to 0.0 V *vs*. Ag/AgCl without H_2O_2 and **(B)** CV curves at different scan rates of 10-100 mV/s for PPy-GO-AuNPs/GCE for same PBS solution in presence of H_2O_2. (for clarity, the CV windows of scan rate are extended in the figures)

Similarly, **Fig. 6 [A]** shows CV curves for PPy-GO-AuNPs/GCE in 0.1 M PBS solution at pH 7 in presence of different H_2O_2 concentrations. The reduction peak current (Ipc) increases with increasing H_2O_2 concentration. The current of Ipc at -0.73 V vs. Ag/AgCl was preferred for quantitative estimation of H_2O_2 as the common electroactive species are reduced at the negative potential. The observed negative shift and broadening in reduction peak potential with an increase in H_2O_2 concentration are inconsistent with earlier reports.[44] The cathodic peak currents at -0.73 V s. Ag/AgCl in the case of nanocomposite for various concentrations of 2.5-25 mM of H_2O_2 is shown in **Fig. 6 [A]**, while the same has been maintained as the background current in absence of H_2O_2. It was used as the calibration curve with a correlation coefficient R^2 value of 0.99703, as represented in **Fig. 6 [B]**. The sensitivity of the nanocomposite was found to be 41.35 µA/mM as obtained from the slope of the calibration curve. The limit of detection (LOD) was defined as 5 µM (at S/N = 3). Relative standard deviation (R.S.D.) diverse from 2.3% to 6.5% (n = 5) for the evaluation of H_2O_2 was followed in the concentration range of 2.5-25 mM. The sensing mechanism of the PPy-GO-AuNPs involves the strong interaction of Au metal immobilization with polypyrrole to form a polymeric film for the enhanced electrocatalytic effect towards H_2O_2.

Presumably, the quinone formation in the polypyrrole complex structure is converted to dihydroxyl form and attached with Au. This structural change is the reason for the reduction of hydrogen peroxide into hydroxyl form which was further confirmed from the proton-electron transfer in the pH effect.

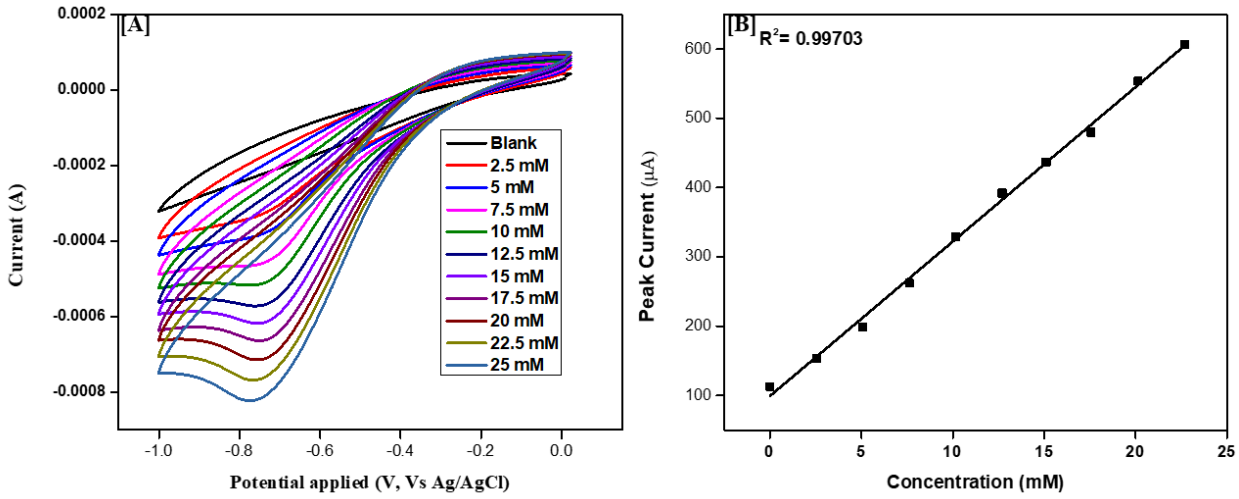

Fig. 6 (A) CV curves of PPy-GO-AuNPs/GCE in 50 mL of 0.1 M PBS Solution (pH 7) with a scan rate of 20 mV/s. CVs at different concentrations of H_2O_2 (2.5 -25 mM); (**B**) The graph shows the linear relationship between the different concentrations of H_2O_2 and reduction current.

3.7. Effect of pH for the determination of H_2O_2

The pH of the PBS solution is one of the major issue for the electrochemical oxidation of H_2O_2 at PPy-GO-AuNPs/GCE. Therefore, pH effect was studied using 0.1 mM H_2O_2 in 0.1 M PBS solution at different pH ranging from 2.0 - 10 at a scan rate of 20 mV/s. By observing the plot of Ip*vs*. pH, the maximum peak current was perceived at pH 7.0 which was selected as optimum pH for present electrochemical studies.

3.8. Amperometric determination of H_2O_2

Amperometric i–t response of PPy-GO-AuNPs/GCE with varying H_2O_2 concentrations (2.5 to 25 mM) into 50 mL of 0.1 M PBS at a working potential of -0.50 V has been shown in **Fig. 7**. The inset of **Fig. 7** shows that an excellent response was obtained after adding H_2O_2 into the PBS solution. Especially, PPy-GO-AuNPs/GCE does not show a significant response in lower

H_2O_2 concentration but shows a sharp response while adding higher concentration i.e. 5, 7.5 and 10 mM of H_2O_2 into PBS solution. These results designate the high catalytic ability of PPy-GO-AuNPs/GCE. The nanocomposite modified GCE electrode exhibits fast electrocatalytic behavior towards H_2O_2 reduction as recorded response time was deliberated as 2s.

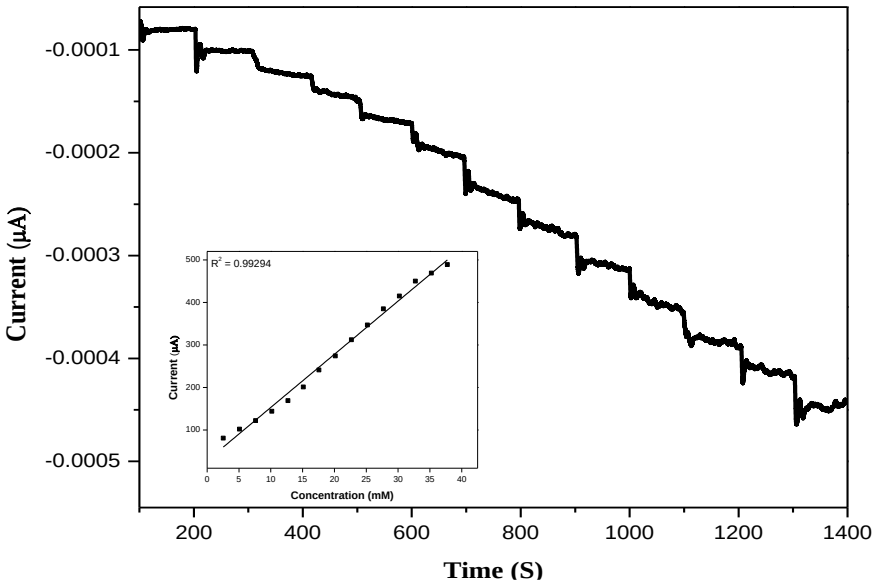

Fig. 7: Amperometric response of the PPy-GO-AuNPs/GCE into the constantly stirred N_2 saturated 50 mL of 0.1 M PBS at a working potential of -0.50 V.

As shown in Fig. 7, the PPy-GO-AuNPs/GCE shows a better and stable amperometric current response for H_2O_2 between the linear concentration range of 2.5 to 25 mM. The estimated sensitivity and LOD for the proposed nanocomposite sensor were found to be 41.35 µA μM^{-1} cm^{-2} and 5 µM (at S/N = 3) respectively. To display the advancement and also to determine the novelty of the developed nanocomposite-based sensor, a comparative study was carried out as summarized in **Table 1**. The data shown in **Table 1** reflects that the developed H_2O_2 sensor exhibits higher sensitivity, low LOD, and wider linear response range for H_2O_2 as compared to the reported values in the literature.

Table 1 Sensitivity, LOD and linear range of different non-enzymatic H_2O_2 sensors

	Performance	References

Chemically modified electrode	Sensitivity	LOD (μM)	Liner range (μM)	
Graphene-AgNPLs	-	3	0.02–10 10^{-3}	[45]
PPy/PB Nanowire	-	-	0.2 - 7.210^{-3}	[46]
PPy/GENS/Au	32 μA mM^{-1} cm^{-2}	-	1-10 10^{-3}	[47]
PPyNPT–Ag	-	1.8	0.01 mM to 3.01 10^{-3}	[12]
Au–graphene	-	0.32	1×10^{-3} to 0.32$10^{-3}$	[48]
AgNPs–rGO/GCE	-	4.3	0.1–70 10^{-3}	[49]
PAA/Au-SPE electrode	899 μA mM^{-1} cm^{-2}	2	-	[50]
Nf/Pd@Ag/rGO-NH_2/GC	1307.46 μA mM^{-1} cm	0.7	0.002-19.500 10^{-3}	[51]
CNT/Fe_3O_4/Au	5.732×10^{-5} μA mM^{-1} cm^{-2}	3.7×10^{-3}	1.2-21.6	[52]
AQGC/GCE	64 nA μM^{-1}	7.3	50-450.	[52]
Nafion-nanoparticle-TiO_2	-	3.1×10^{-7} mol/ L^{-1}	1.6×10^{-5} –3.1×10^{-2} mol/ L	[53]
3D-MoS2–PANI–Ag nanocubes	-	1.1×10^{-9} mol/ L^{-1}	3.3×10^{-9} –0.45×10^{-3} mol/ L	[54]
AuNPs@MWCNTs	-	4.2×10^{-16} mol/ L^{-1}	1.4×10^{-15}–1.12×10^{-9} mol/ L	[55]
Polypyrrole doped by Sodium dodecyl sulfate and CeO_2 nanoparticle	-	1.2×10^{-16} mol/ L^{-1}	5×10^{-16}– 5×10^{-5} mol L^{-1}	[56]
TaOx		1 nm		[57]
GdOx Membrane		1 μM		[58]
PPy-GO-Au NPs	**41.35 (μA/mM)**	**5**	**2.5-25 10^{-3}**	**Present study**

3.9. Repeatability, reproducibility, and stability

The repeatability and reproducibility results of the prepared sensor were carried out. The repeatability of the sensor was determined using 1 mM H_2O_2 which exhibits fairly good results. The RSD was 1.22% for 10 successive assays. Five different modified electrodes were made under similar conditions and relative standard deviation (RSD) was found to be 2.14% for the current response of 1 mM H_2O_2 which confirms that the results can be reproduced. To study the stability of the developed nanocomposite sensor material, experiments were performed with PPy-GO-AuNPs/GCE for 1 mM H_2O_2 for several days at pH 7 PBS using the same parameters as mentioned above. It was found that the developed sensor still retained 94% of its initial current response even after more than 30 days. The stability of the sensor means the stability of the components and in

the present case, PPy plays an important role in immobilizing GO and Au NPs on the electrode surface providing stable nanostructured material.[59]

The effect of electroactive interfering species was also studied for the developed nanocomposite materials PPy-GO-AuNPs/GCE. The Amperometric performance of PPy-GO-AuNPs/GCE for subsequent addition of 0.1 mM of each i.e. H_2O_2, glucose, ascorbic acid, ethanol, and uric acid into the 0.1 M PBS at pH 7 has been shown in **Fig. S7.** It shows the superior selectivity of developed nanocomposite PPy-GO-AuNPs/GCE for H_2O_2 detection.

3.10. Determination of H_2O_2 in real samples

The developed PPy-GO-AuNPs/GCE was also used for the estimation of H_2O_2 in real milk samples from the practical application point of view as H_2O_2 sensor. Keeping the similar experimental parameters as mentioned above, the amperometric *i-t* response was obtained for the recognition of H_2O_2 comprising real milk samples. The real milk sample (10 mL) was first diluted with pH 7.0 to condense the sample matrix effect. Then, a known concentration of H_2O_2 (0.1 mM) comprising milk samples was used for the sensing investigation of the real samples. The investigations were carried out at fix interval of (100 s) to get the amperometric response. The recovery results of H_2O_2 are mentioned in **Table 2**. The recovery percentage of H_2O_2 was estimated by using a standard addition system and was found to be 96.0-100.6% in the present case. The PPy-GO-AuNPs/GCE exhibits excellent and adequate recovery of H_2O_2 in milk.

Table 2 Real sample analysis of the PPy-GO-AuNPs composites modified GCE for the detection of H_2O_2 in raw milk samples (n = 3).

Real sample	Added (μM)	Found (μM)	Recovery (%)
Milk	R	20	-
	R+S1(50)	68	96.0
	R+S2(75)	94	98.6
	R+S3(100)	120.6	100.6

4. Conclusions

In conclusion, an amperometric H_2O_2 sensor has been established using PPy-GO-AuNPs modified electrode. The UV–vis spectrum, FT-IR, Raman spectroscopy SEM-EDX, observations confirm the formation of PPy-GO-AuNPs nanocomposites. Further, it was compared with the

unmodified electrode, and the overall results suggest that PPy-GO-AuNPs/GCE electrode exhibits an improved catalytic activity and ultra-high sensitivity for the detection of H_2O_2 along with lower LOD. The real milk samples analysis reveals that the synthesized PPy-GO-AuNPs nanocomposite is more applicable for real sample analysis. Also, the fabricated PPy-GO-AuNPs modified electrode shows a higher selectivity towards H_2O_2 detection in the presence of potentially interfering compounds.

Author Contribution Statement

D. Mathivanan: Writing- Original draft preparation, **K.S. ShaliniDevi**: Data collection and Editing, **G. Sathiyan**: Data collection and editing, **Ankit Tyagi**: Data collection and editing, **V. A. O. P. da Silva**: Reviewing and Editing, **B. C. Janegitz**: Reviewing and Editing, **Jai Prakash**: Supervision, Conceptualization, Methodology and **R. K. Gupta**: Supervision,Reviewing and Editing

Acknowledgment
The author (J P) thank the Department of Science and Technology (DST), New Delhi, India for the prestigious INSPIRE Faculty award [INSPIRE/04/2015/002452 (IFA15-MS-57)] along with research grant.

Conflicts of interest

There are no conflicts of interest to declare.

References

[1] Du X, Chen Y, Dong W, Han B, Liu M, Chen Q, et al. A nanocomposite-based electrochemical sensor for non-enzymatic detection of hydrogen peroxide. Oncotarget. 2017;8:13039-47.

[2] Roy A, Chen Y-P, Qiu JT, Maikap S. Sarcosine Prostate Cancer Biomarker Detection by Controlling Oxygen in NiOx Membrane on Vertical Silicon Nanowires in Electrolyte–Insulator–Nanowire Structure. Analytical Chemistry. 2020;92:8064-71.

[3] Yang Y-Q, Xie H-L, Tang J, Tang S, Yi J, Zhang H-L. Design and preparation of a non-enzymatic hydrogen peroxide sensor based on a novel rigid chain liquid crystalline polymer/reduced graphene oxide composite. RSC Advances. 2015;5:63662-8.

[4] Chen LC, Yu Z, Hiraoka K. Vapor phase detection of hydrogen peroxide with ambient sampling chemi/chemical ionization mass spectrometry. Analytical Methods. 2010;2:897-900.
[5] Zhang Y, Jiao Z, Xu W, Fu Y, Zhu D, Xu J, et al. Design, synthesis and properties of a reactive chromophoric/fluorometric probe for hydrogen peroxide detection. New Journal of Chemistry. 2017;41:3790-7.
[6] Song M, Wang J, Chen B, Wang L. A Facile, Nonreactive Hydrogen Peroxide (H2O2) Detection Method Enabled by Ion Chromatography with UV Detector. Analytical Chemistry. 2017;89:11537-44.
[7] Zhao C, Cui H, Duan J, Zhang S, Lv J. Self-Catalyzing Chemiluminescence of Luminol-Diazonium Ion and Its Application for Catalyst-Free Hydrogen Peroxide Detection and Rat Arthritis Imaging. Analytical Chemistry. 2018;90:2201-9.
[8] Lu X, Xiao X, Li Z, Xu F, Tan H, Sun L, et al. A novel nonenzymatic hydrogen peroxide sensor based on three-dimensional porous Ni foam modified with a Pt electrocatalyst. Analytical Methods. 2014;6:235-41.
[9] Li X, Liu Y, Zheng L, Dong M, Xue Z, Lu X, et al. A novel nonenzymatic hydrogen peroxide sensor based on silver nanoparticles and ionic liquid functionalized multiwalled carbon nanotube composite modified electrode. Electrochimica Acta. 2013;113:170-5.
[10] Wang L, Wu T, Wu H, Zhong J, Wang N, Wang R. A novel non-enzymatic hydrogen peroxide sensor based on Co:ZnO modified electrodes. Progress in Natural Science: Materials International. 2018;28:24-7.
[11] Prakash J, Sun S, Swart HC, Gupta RK. Noble metals-TiO2 nanocomposites: From fundamental mechanisms to photocatalysis, surface enhanced Raman scattering and antibacterial applications. Applied Materials Today. 2018;11:82-135.
[12] Ding J, Zhang K, Wei G, Su Z. Fabrication of polypyrrole nanoplates decorated with silver and gold nanoparticles for sensor applications. RSC Advances. 2015;5:69745-52.
[13] Feng X, Huang H, Ye Q, Zhu J-J, Hou W. Ag/Polypyrrole Core−Shell Nanostructures: Interface Polymerization, Characterization, and Modification by Gold Nanoparticles. The Journal of Physical Chemistry C. 2007;111:8463-8.
[14] Moozarm Nia P, Lorestani F, Meng WP, Alias Y. A novel non-enzymatic H2O2 sensor based on polypyrrole nanofibers–silver nanoparticles decorated reduced graphene oxide nano composites. Applied Surface Science. 2015;332:648-56.

[15] Prakash J, Pivin JC, Swart HC. Noble metal nanoparticles embedding into polymeric materials: From fundamentals to applications. Advances in Colloid and Interface Science. 2015;226:187-202.
[16] Prakash J, Tripathi A, Khan SA, Kumar S, Singh F, Tripathi JK, et al. Investigation of swift heavy ion-induced mixing in metal/polymer systems. Radiation Effects and Defects in Solids. 2011;166:682-8.
[17] Mathpal MC, Kumar P, Kumar S, Tripathi AK, Singh MK, Prakash J, et al. Opacity and plasmonic properties of Ag embedded glass based metamaterials. RSC Advances. 2015;5:12555-62.
[18] Kumar P, Mathpal MC, Prakash J, Hamad S, Rao SV, Viljoen BC, et al. Study of Tunable Plasmonic, Photoluminscence, and Nonlinear Optical Behavior of Ag Nanoclusters Embedded in a Glass Matrix for Multifunctional Applications. physica status solidi (a). 2019;216:1800768.
[19] Prakash J, Kumar P, Harris RA, Swart C, Neethling JH, van Vuuren AJ, et al. Synthesis, characterization and multifunctional properties of plasmonic Ag–TiO2nanocomposites. Nanotechnology. 2016;27:355707.
[20] Prakash J, Kumar V, Kroon RE, Asokan K, Rigato V, Chae KH, et al. Optical and surface enhanced Raman scattering properties of Au nanoparticles embedded in and located on a carbonaceous matrix. Physical Chemistry Chemical Physics. 2016;18:2468-80.
[21] Prakash J, Tripathi A, Gautam S, Chae KH, Song J, Rigato V, et al. Phenomenological understanding of dewetting and embedding of noble metal nanoparticles in thin films induced by ion irradiation. Materials Chemistry and Physics. 2014;147:920-4.
[22] Prakash J, Tripathi A, Rigato V, Pivin JC, Tripathi J, Chae KH, et al. Synthesis of Au nanoparticles at the surface and embedded in carbonaceous matrix by 150 keV Ar ion irradiation. Journal of Physics D: Applied Physics. 2011;44:125302.
[23] Ouyang Z, Li J, Wang J, Li Q, Ni T, Zhang X, et al. Fabrication, characterization and sensor application of electrospun polyurethane nanofibers filled with carbon nanotubes and silver nanoparticles. Journal of Materials Chemistry B. 2013;1:2415-24.
[24] Janegitz BC, Medeiros RA, Rocha-Filho RC, Fatibello-Filho O. Direct electrochemistry of tyrosinase and biosensing for phenol based on gold nanoparticles electrodeposited on a boron-doped diamond electrode. Diamond and Related Materials. 2012;25:128-33.

[25] Campanhã Vicentini F, Garcia LLC, Figueiredo-Filho LCS, Janegitz BC, Fatibello-Filho O. A biosensor based on gold nanoparticles, dihexadecylphosphate, and tyrosinase for the determination of catechol in natural water. Enzyme and Microbial Technology. 2016;84:17-23.
[26] Raj CR, Okajima T, Ohsaka T. Gold nanoparticle arrays for the voltammetric sensing of dopamine. Journal of Electroanalytical Chemistry. 2003;543:127-33.
[27] Singh RK, Kumar R, Singh DP. Graphene oxide: strategies for synthesis, reduction and frontier applications. RSC Advances. 2016;6:64993-5011.
[28] Lin Y-P, Ksari Y, Prakash J, Giovanelli L, Valmalette J-C, Themlin J-M. Nitrogen-doping processes of graphene by a versatile plasma-based method. Carbon. 2014;73:216-24.
[29] Yang X, Zhang G, Prakash J, Chen Z, Gauthier M, Sun S. Chemical vapour deposition of graphene: layer control, the transfer process, characterisation, and related applications. International Reviews in Physical Chemistry. 2019;38:149-99.
[30] Wang L, Wu A, Wei G. Graphene-based aptasensors: from molecule–interface interactions to sensor design and biomedical diagnostics. Analyst. 2018;143:1526-43.
[31] Janegitz BC, Silva TA, Wong A, Ribovski L, Vicentini FC, Taboada Sotomayor MdP, et al. The application of graphene for in vitro and in vivo electrochemical biosensing. Biosensors and Bioelectronics. 2017;89:224-33.
[32] Buitrago-Sierra R, García-Fernández MJ, Pastor-Blas MM, Sepúlveda-Escribano A. Environmentally friendly reduction of a platinum catalyst precursor supported on polypyrrole. Green Chemistry. 2013;15:1981-90.
[33] Yalçınkaya S, Çakmak D. Electrochemical Synthesis of Poly (pyrrole-co-[Cu (salabza)]): its Electrocatalytic Activity Towards the Oxidation of Catechol, Hacettepe J. Biol Chem. 2016;44:425-34.
[34] Qian T, Yu C, Wu S, Shen J. A facilely prepared polypyrrole–reduced graphene oxide composite with a crumpled surface for high performance supercapacitor electrodes. Journal of Materials Chemistry A. 2013;1:6539-42.
[35] Mikoliūnaitė L, Kubiliūtė R, Popov A, Voronovič J, Šakirzanovas S, Ramanavičienė A, et al. Development of gold nanoparticle-polypyrrole nanocomposites. AUKSO NANODALELIŲ IR POLIPIROLO NANODARINIŲ SINTEZĖ IR TYRIMAS. 2014;25:63-9.

[36] Patil DS, Shaikh JS, Pawar SA, Devan RS, Ma YR, Moholkar AV, et al. Investigations on silver/polyaniline electrodes for electrochemical supercapacitors. Physical Chemistry Chemical Physics. 2012;14:11886-95.
[37] Dhibar S, Das CK. Silver nanoparticles decorated polypyrrole/graphene nanocomposite: A potential candidate for next-generation supercapacitor electrode material. Journal of Applied Polymer Science. 2017;134.
[38] Reddy KR, Sin BC, Ryu KS, Kim J-C, Chung H, Lee Y. Conducting polymer functionalized multi-walled carbon nanotubes with noble metal nanoparticles: Synthesis, morphological characteristics and electrical properties. Synthetic Metals. 2009;159:595-603.
[39] Biswas S, Drzal LT. Multilayered Nanoarchitecture of Graphene Nanosheets and Polypyrrole Nanowires for High Performance Supercapacitor Electrodes. Chemistry of Materials. 2010;22:5667-71.
[40] Lim SP, Pandikumar A, Lim YS, Huang NM, Lim HN. In-situ electrochemically deposited polypyrrole nanoparticles incorporated reduced graphene oxide as an efficient counter electrode for platinum-free dye-sensitized solar cells. Scientific Reports. 2014;4:5305.
[41] Xing S, Zhao G. One-step synthesis of polypyrrole–Ag nanofiber composites in dilute mixed CTAB/SDS aqueous solution. Materials Letters. 2007;61:2040-4.
[42] Xu C, Sun J, Gao L. Synthesis of novel hierarchical graphene/polypyrrole nanosheet composites and their superior electrochemical performance. Journal of Materials Chemistry. 2011;21:11253-8.
[43] Karuppiah C, Palanisamy S, Chen S-M, Veeramani V, Periakaruppan P. A novel enzymatic glucose biosensor and sensitive non-enzymatic hydrogen peroxide sensor based on graphene and cobalt oxide nanoparticles composite modified glassy carbon electrode. Sensors and Actuators B: Chemical. 2014;196:450-6.
[44] Li Y, Zhang Y, Zhong Y, Li S. Enzyme-free hydrogen peroxide sensor based on Au@Ag@C core-double shell nanocomposites. Applied Surface Science. 2015;347:428-34.
[45] Li L, Du Z, Liu S, Hao Q, Wang Y, Li Q, et al. A novel nonenzymatic hydrogen peroxide sensor based on MnO2/graphene oxide nanocomposite. Talanta. 2010;82:1637-41.
[46] Lin M, Yang J, Cho M, Lee Y. Hydrogen peroxide detection using a polypyrrole/Prussian blue nanowire modified electrode. Macromolecular Research. 2011;19:673-8.

[47] Yu Y, Chen J, Zhou J. Enzyme-free electroreduction of hydrogen peroxide at polypyrrole/graphene/au microelectrode based on three-electrode-system array. 2013 13th IEEE International Conference on Nanotechnology (IEEE-NANO 2013): IEEE; 2013. p. 1067-70.
[48] Zhu W, Chen T, Ma X, Ma H, Chen S. Highly sensitive and selective detection of dopamine based on hollow gold nanoparticles-graphene nanocomposite modified electrode. Colloids and Surfaces B: Biointerfaces. 2013;111:321-6.
[49] Golsheikh AM, Huang NM, Lim HN, Zakaria R. One-pot sonochemical synthesis of reduced graphene oxide uniformly decorated with ultrafine silver nanoparticles for non-enzymatic detection of H2O2 and optical detection of mercury ions. RSC Advances. 2014;4:36401-11.
[50] Zamfir L-G, Rotariu L, Marinescu VE, Simelane XT, Baker PGL, Iwuoha EI, et al. Non-enzymatic polyamic acid sensors for hydrogen peroxide detection. Sensors and Actuators B: Chemical. 2016;226:525-33.
[51] Guler M, Turkoglu V, Bulut A, Zahmakiran M. Electrochemical sensing of hydrogen peroxide using Pd@Ag bimetallic nanoparticles decorated functionalized reduced graphene oxide. Electrochimica Acta. 2018;263:118-26.
[52] Thandavan K, Gandhi S, Nesakumar N, Sethuraman S, Rayappan JBB, Krishnan UM. Hydrogen peroxide biosensor utilizing a hybrid nano-interface of iron oxide nanoparticles and carbon nanotubes to assess the quality of milk. Sensors and Actuators B: Chemical. 2015;215:166-73.
[53] Ye R, Huang L, Qiu B, Song Z, Lin Z, Chen G. Cathodic electrochemiluminescent behavior of luminol at nafion–nano-TiO2 modified glassy carbon electrode. Luminescence. 2011;26:531-5.
[54] Ou X, Tan X, Liu X, Chen H, Fan Y, Chen S, et al. A cathodic luminol-based electrochemiluminescence biosensor for detecting cholesterol using 3D-MoS2–PANI nanoflowers and Ag nanocubes for signal enhancement. RSC Advances. 2015;5:66409-15.
[55] Cao Y, Yuan R, Chai Y, Mao L, Niu H, Liu H, et al. Ultrasensitive luminol electrochemiluminescence for protein detection based on in situ generated hydrogen peroxide as coreactant with glucose oxidase anchored AuNPs@MWCNTs labeling. Biosensors and Bioelectronics. 2012;31:305-9.

[56] Karimi A, Husain SW, Hosseini M, Azar PA, Ganjali MR. Rapid and sensitive detection of hydrogen peroxide in milk by Enzyme-free electrochemiluminescence sensor based on a polypyrrole-cerium oxide nanocomposite. Sensors and Actuators B: Chemical. 2018;271:90-6.
[57] Chakrabarti S, Panja R, Roy S, Roy A, Samanta S, Dutta M, et al. Evolution of resistive switching mechanism through H2O2 sensing by using TaOx-based material in W/Al2O3/TaOx/TiN structure. Applied Surface Science. 2018;433:51-9.
[58] Kumar P, Maikap S, Qiu J-T, Jana S, Roy A, Singh K, et al. Detection of pH and Enzyme-Free H2O2 Sensing Mechanism by Using GdOxMembrane in Electrolyte-Insulator-Semiconductor Structure. Nanoscale Research Letters. 2016;11:434.
[59] Wu B, Zhao N, Hou S, Zhang C. Electrochemical Synthesis of Polypyrrole, Reduced Graphene Oxide, and Gold Nanoparticles Composite and Its Application to Hydrogen Peroxide Biosensor. Nanomaterials (Basel, Switzerland). 2016;6.